Available online at www.sciencedirect.com
ScienceDirect
Nuclear Physics B Proceedings Supplement 00 (2012) 1–6
Nuclear Physics B Proceedings Supplement

Final State Interactions and Polarization Observables in the Reaction pp → pKΛ

M. Roeder and J. Ritman for the COSY-TOF Collaboration

Institut fuer Kernphysik, Forschungszentrum Juelich, D-52428 Juelich, Germany

Abstract

Hyperon-Nucleon (YN) interactions are ideally suited to study the role of strangeness in hadron physics. The breaking of the SU(3) flavor symmetry beyond the mass splitting can also be tested. Due to the lack of high quality hyperon beams, final state interactions in hyperon production reactions are a compelling tool for these studies. Recent measurements of the reaction $pp \to pK\Lambda$ with polarized beam using the COSY-TOF detector allow for the determination of the spin triplet $p\Lambda$ scattering length, which is a fundamental parameter of the $p\Lambda$ interaction. Furthermore, the polarized beam together with the self analyzing decay of the polarized Λ give access to a plethora of observables for studies of the hyperon production mechanism close to threshold. Recent experimental results on the scattering length and the Λ depolarization are presented.

Keywords: Strangeness, Hyperon-Nucleon interactions, Final State Interactions, Lambda Depolarization

1. Introduction

Studies of Hyperon-Nucleon (YN) interactions are important to understand the role of strangeness in hadron physics. They are also an important prerequisite to describe hypernuclei and the equation of state of neutron stars. Furthermore, it is interesting to check if the breaking of SU(3) flavor symmetry in QCD also appears in the interaction itself. This would imply differences between YN and NN interactions beyond the obvious mass effects.

From the theoretical point of view YN interactions are described in the framework of meson exchange models by potential models and chiral effective field theory. Their predictions for the spin triplet and spin singlet $p\Lambda$ scattering length are consistent through the need to predict sufficient binding energy for the hypertriton. Experimentally, final state interactions in hyperon production reactions like $pp \to pK\Lambda$ might be the most important option to measure these quantities. In 2004 Gasparyan et. al. proposed a method[1] to determine the spin triplet scattering length from the shape of the $p\Lambda$ invariant mass spectrum in combination with the K^+ analyzing power. Here, we present our recent attempt to apply this method to data at a beam momentum of $p_{\mathrm{beam}} = 2.95\,\mathrm{GeV}/c$.

Another interesting aspect is the role of strangeness for the polarization of the Λ in the production mechanism. The polarized proton beam and the self analyzing decay of the Λ allow to determine the spin transfer coefficient D_{NN}. In the framework of the Laget model this quantity is sensitive to K or π exchange in the production mechanism. Close to threshold this quantity has only been measured by the DISTO[2] collaboration before.

2. Experimental Setup

The COSY-TOF fixed target experiment, depicted in Fig. 1, measures the reaction $pp \to pK\Lambda$ with complete kinematic acceptance and high geometrical precision. Because the momenta of the final state particles are only in the order of a few hundred MeV/c it is essential to keep the mass of the detector as low as possible to minimize multiple scattering. Therefore, a particle only traverses material with a radiation length of $X/X_0 \approx 0.02$ before it arrives at the segmented scintillators at the inner side of the vacuum vessel. These

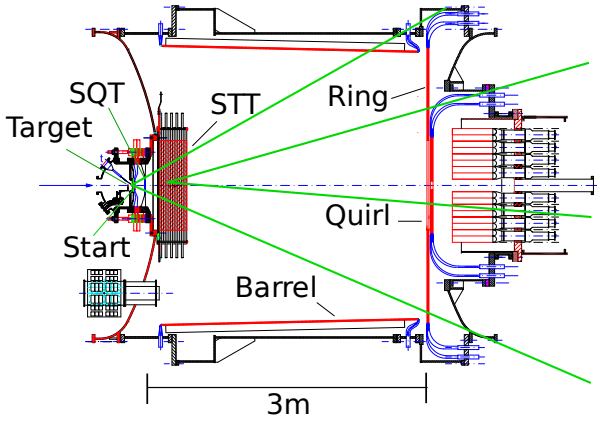

Figure 1: A CAD drawing of the COSY-TOF Detector. The green lines indicate the tracks of the final state particles in the $pp \to pk\Lambda$ reaction. Figure from Ref. [3].

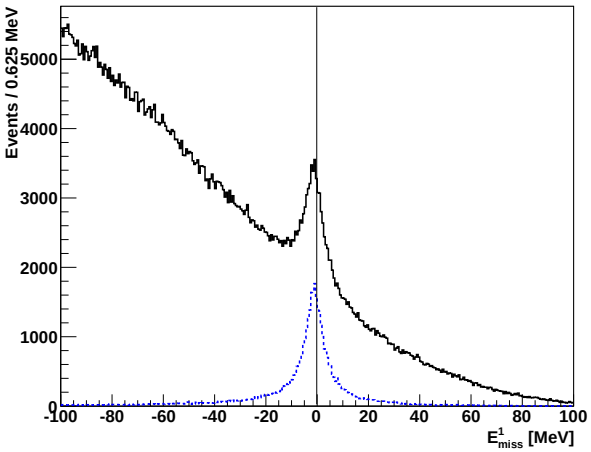

Figure 2: The missing energy in the primary vertex before the kinematic fit. A clear signal peak can be seen on the background continuum (solid). The event selection extracts the peak (dashed).

scintillator systems (Quirl, Ring and Barrel) deliver the stop signal for the time of flight measurement and are complemented by two segmented scintillators of 1 *mm* thickness 1 cm behind the target that provide the start signal. The timing resolution is $\sigma \approx 300\,\mu$s and the flight path is approximately 3 m if a particle hits the end cap.

Tracking is done with a silicon disc with segmented readout cathodes (SQT) in 2.5 cm distance behind the target and most importantly with the Straw Tube Tracker (STT)[4]. This system consists of 2704 straws of 1.05 m length and 10 mm diameter. The 26 straw layers are combined into densely packed double layers that are arranged in three orientations for three dimensional track information. Despite their mylar walls being only 20 μm thick the straws are self supporting due to their operation under 1.2 bar overpressure inside the COSY-TOF vacuum. Therefore, massive support structures are not needed and the straws are mounted in frames made of Rohacell® integral foam. The first double layer has a distance of $\approx$ 270 mm to the target. Therefore, the primary vertex and the delayed hyperon vertices can be reconstructed.

3. Event Reconstruction and Selection

For all triggered events with a track multiplicity of

$$n_{\text{tracks}} = 4 \tag{1}$$

the tracks are combined into two vertices. A minimum distance between secondary and primary vertex of

$$d = 3\,\text{cm} \tag{2}$$

is required to reject background events with four primary tracks like $pp \to pp\pi^+\pi^-$. For the highest possible reconstruction precision and to reject $pp \to pK\Sigma^0 \to pk\Lambda\gamma$ events a kinematic fit is performed. As the undetected photon in this physical background reaction carries away only $\approx$ 70 MeV the event topology is similar to the signal. The precision of the COSY accelerator[5] is so high that the initial state can be assumed to be known. This reduces the number of free parameters to 11. With two overconstraints, these are fit directly to the isochrones of the straw measurements. We set a threshold on the reduced χ^2

$$\chi^2_{\text{Kinfit}}/\text{NDF} < 5. \tag{3}$$

The primary p and K identification is done by comparing the χ^2_{Kinfit} of either mass hypotheses. Studies with Monte Carlo (MC) generated events show that this reduces the physical background to less then 5%. The pΛ invariant mass resolution is determined to be $\sigma_m \approx 1.1\,\text{MeV}/c^2$[3]. To additionally reduce instrumental background a minimum angle between the secondary proton and lambda is demanded:

$$\measuredangle(\vec{p}_p, \vec{p}_\Lambda) > 0.15\,\text{mrad} \tag{4}$$

To show the effectiveness of the event selection the missing energy in the primary vertex before the kinematic fit is shown. In black for all events with $d > 1$ cm and in blue for all events that fulfill Eqs. 1-4. It can be seen that only events in the signal peak around 0 MeV are selected. A total of 42.000 Events is obtained.

The Dalitz plot of the selected event sample is shown in Fig. 3. A prominent cusp is visible in the $p\Lambda$ invariant

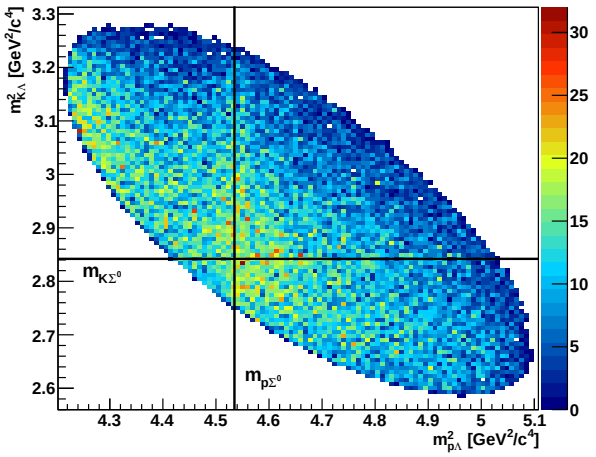

Figure 3: The Dalitz plot of the selected event sample. It is not corrected for acceptance. The black lines mark the $p\Sigma^0$ and K^0 threshold, respectively. The enhancements at these positions stem from coupled channel effects; final state interactions are visible close to the $p\Lambda$ threshold.

mass spectrum at the $p\Sigma^0$ threshold. This comes from a $p\Lambda$-$p\Sigma^0$ coupled channel effect. Because this plays an important role in hypernuclear physics it will be subject to further studies. However, this is beyond the scope of this work. The structure underneath can be explained by final state interactions close to the $p\Lambda$ threshold and influences of $N^*(1710)$ or (1720) resonances.

4. Polarization Observables

The Λ polarization (P_N) can be determined from the asymmetry of its decay products. With the weighted sums method[6] we obtain $+10\,\%$ for backward and $-10\,\%$ for forward Λs. The influence of the 61 % transversely polarized proton beam on this polarization can be determined by dividing the event sample into four subsamples. Two subsamples have the beam spin oriented upwards and the quantization axis of Λ polarization in the same ($\uparrow\uparrow$) or opposite ($\uparrow\downarrow$) detector hemispheres, respectively. Another two subsamples are obtained from measurements with the beam spin oriented downwards ($\downarrow\downarrow$, $\downarrow\uparrow$). The polarizations for all four subsamples are given in Fig. 4.

The associated Λ polarizations for opposite beam spin orientations, $\uparrow\uparrow$ with $\downarrow\downarrow$ and $\uparrow\downarrow$ with $\downarrow\uparrow$, are self-consistent within the statistical accuracy. This shows that systematic effects from azimuthal detector asymmetries and differences in up/down beam polarization are below the statistical sensitivity. Differences between opposite orientations of the quantization axis of the beam polarization as well as to the unpolarized case

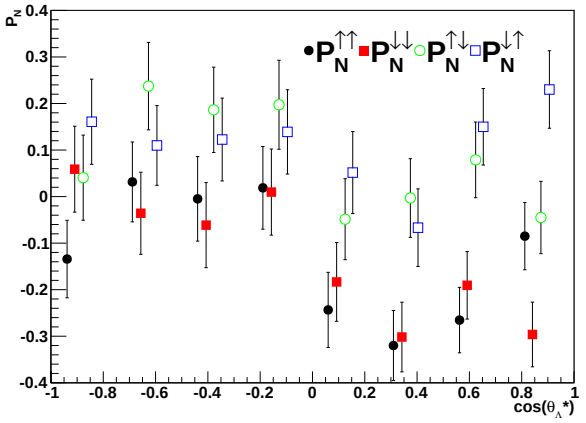

Figure 4: The Lambda polarization for different event samples as described in the text.

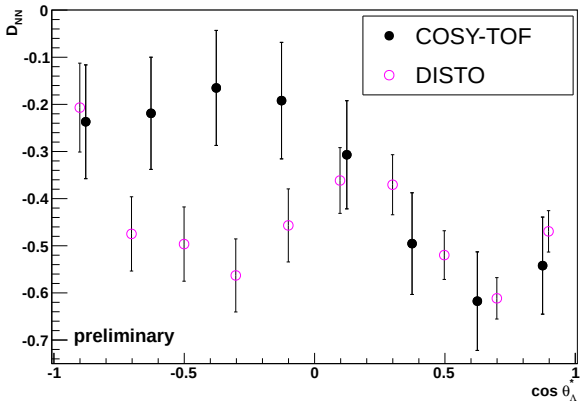

Figure 5: The Lambda depolarization. Our result (solid) in comparison with DISTO[2] (open).

are evident. These differences are quantified by the spin transfer coefficient D_{NN}, also referred to as depolarization. Our result is shown in Fig. 5 together with a measurement of the DISTO collaboration[2]. For forward Λs we obtain $D_{NN} \approx -0.6$ and find an agreement between both experiments. For backward Λs the absolute value of D_{NN} decreases and our result is significantly closer to $D_{NN} = 0$ than the DISTO data.

In the framework of the Laget Model[7] the $pK\Lambda$ production mechanism is described with K and π exchange. In Fig. 6 the corresponding Feynman diagrams are shown. The given spin and parity structure at the Λ production vertex require requires a spin flip in case of K exchange, corresponding to $D_{NN} = -1$. Because π exchange does not require a spin flip the depolarization is $D_{NN} = +1$ for this process[2]. In this context our result can be interpreted as predominant K exchange with modest contributions of π exchange. The decreasing

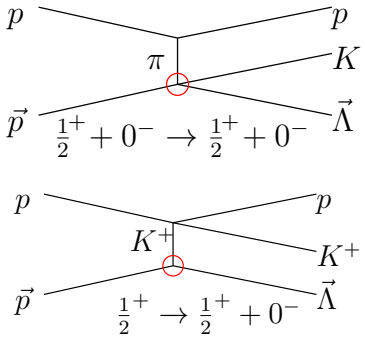

Figure 6: K and π exchange diagrams of the Laget Model[7, 2]. The spin and parity of the ingoing and outgoing particles at the Λ production vertex are shown.

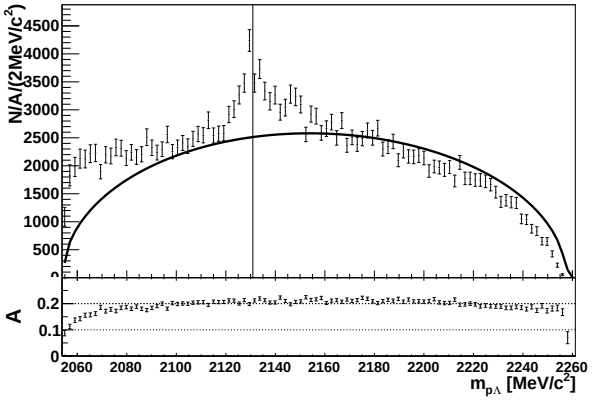

Figure 7: The proton lambda invariant mass spectrum. The vertical line marks the cusp position at the $p\Sigma^0$ threshold. A phasespace distribution is drawn (solid line) to guide the eye. Figure from Ref. [3].

D_{NN} for backward Λs is expected from gluon exchange models for high energy data that predict a connection of the Λ with the unpolarized target proton at $\cos(\theta^*_\Lambda) = -1$ as opposed to a connection with the polarized beam proton at $\cos(\theta^*_\Lambda) = +1$.

Because the two experiments have contradictory results on that matter it is important to substantiate our measurement with better statistics. Furthermore, N^* resonances are neglected in the Laget Model, thus it is also important to measure and compare data at different beam momenta.

5. Final State Interactions

In Fig. 7 the $p\Lambda$ invariant mass spectrum is shown. It is corrected for the detector acceptance (A) that is shown on the bottom of the figure. A was determined by MC simulated events. It is nearly constant for the whole spectrum but drops down by 50% near the threshold. In this region the angle between the primary proton

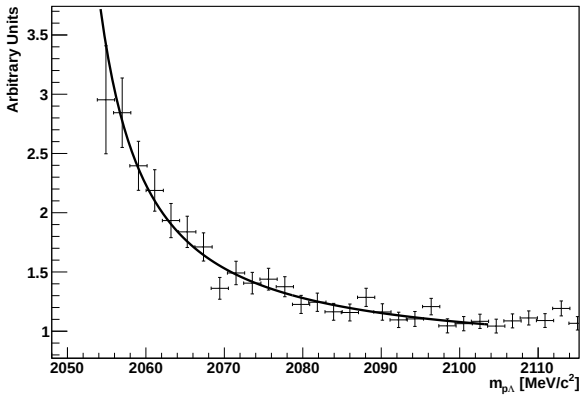

Figure 8: The $p\Lambda$ scattering amplitude. The vertical line marks the cusp position at the $p\Sigma^0$ threshold. An arbitrarily scaled phasespace distribution is shown to guide the eye. Figure from Ref. [3].

and the Λ, thus between both protons becomes too small for a proper reconstruction of both tracks. An arbitrarily scaled phasespace distribution is drawn to guide the eye. The cusp is visible at the $p\Sigma^0$ threshold is marked with the vertical line. The enhancement close to threshold comes from final state interactions.

From dividing the corrected spectrum by the phasespace distribution the $p\Lambda$ scattering amplitude $|A_{\text{eff}}|^2$ is obtained in arbitrary units as shown in Fig. 8. Because spin singlet and spin triplet $p\Lambda$ scattering contributes with unknown weigths it is referred to as effective amplitude. Following the method described in Ref. [1] we fit a specially parametrized exponential function, convoluted with the detector resolution to the amplitude. From that we obtain the effective scattering length of $a_{\text{eff}} = (-1.28 \pm 0.01 \pm 0.03)$ fm.

The ability to determine a_{eff} without knowledge of the absolute scale of $|A_{\text{eff}}|^2$ enables one to determine the spin triplet scattering length, too. For that one uses the fact that for the spin triplet scattering amplitude it holds

$$|A_{\text{eff}}(m_{p\Lambda})|^2 \propto p_1^1(m_{p\Lambda}) \cdot |A_{\text{eff}}(m_{p\Lambda})|^2. \qquad (5)$$

Here, p_1^1 is the strength the lowest order symmetric contribution to the K analyzing power (A_N), parametrized by an associated Legendre polynomial of order and degree one (P_1^1). This proportionality can be explained by treating the $p\Lambda$ system as quasi particle in the final state $pp \rightarrow K\{p\Lambda\}$. The symmetric contribution to A_N stems from S and P wave interference of the K angular momentum relative to $\{p\Lambda\}$. Close to threshold it is a good assumption that the $p\Lambda$ internal angular momentum is zero. Under this condition one can show[1] that only spin triplet scattering contributes to K P-wave and therefore p_1^1.

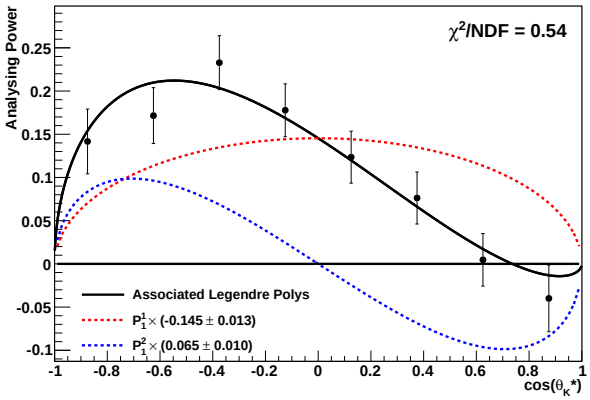

Figure 9: The K analyzing power (A_N) as a function of cos θ of the K in the CMS. A partial wave analysis (solid line) up to K D-wave is fit to the data. The two contributing symmetric and asymmetric associated Legendre polynomials are also shown (dashed lines). Figure from Ref. [3].

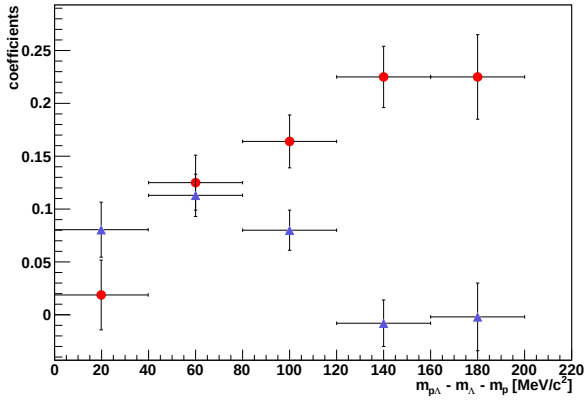

Figure 10: The coefficients of the partial wave analysis of the K analyzing power as a function of the $p\Lambda$ invariant mass. Figure from Ref. [3].

In Fig. 9 A_N is shown for the full $m_{p\Lambda}$ range. A partial wave analysis up to K D-wave is fit to the data. Next to the symmetric contribution P_1^1 an asymmetric Legendre polynomial P_1^2, representing K S- and D-wave interference, is needed to describe the data. The reduced χ of 0.54 justifies the exclusion of higher order partial waves. From Eq. (5) it is clear that the coefficient p_1^1 has to be determined as a function of $m_{p\Lambda}$ in the region close to threshold.

The coefficients of both Legendre polynomials $-p_1^1$ (circles) and p_1^2 (triangles) as a function of $m_{p\Lambda}$ are given in Fig. 10. The decreasing of p_1^2 for higher $m_{p\Lambda}$ shows how the K momentum becomes insufficient for D-wave interference. The symmetric contribution on the other hand is $\approx$ 25 % in the last to bins, thus P wave interference still play a role. Very surprising is the

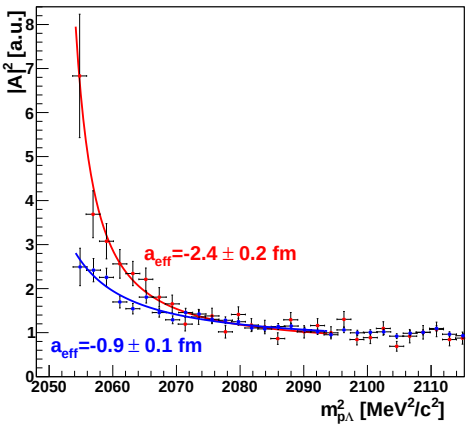

Figure 11: The scattering amplitudes for different regions of the Dalitz plot as explained in the text. The different scattering length reveal the systematic effect of N^* resonances on the measurement.

decreasing of p_1^1 to small $m_{p\Lambda}$ because in the reaction $pp \to \pi d$ with the same selection rules $A_N \approx 25\%$ was measured, close to threshold[8]. With $p_1^1 \approx -0.02 \pm 0.03$ in the first 40 MeV/c^2 the method is not applicable with the statistics that is applied so far.

Because only spin triplet scattering contributes to K P-wave close to threshold, exclusive spin singlet scattering is a possible explanation for that behavior. However, other explanations exist: The four contributing P wave amplitudes could be individually zero or interfere destructively. Furthermore, as only the imaginary part of the partial wave interference contribute to the analyzing power a phase cancellation is possible. Because the viability of those explanations depends heavily on the exact value of p_1^1 close to threshold it is very important to improve the statistics of our data sample.

Another important aspect of the method is the influence of N^* resonances on the shape of $|A|^2$, hence the determined scattering length. For that it is foreseen to measure at several beam momenta. However, the full kinematic acceptance of the detector already allows to divide the Dalitz plot in $m_{k\Lambda}^2$ to create two regions with different distances to the center of the broad resonances centered around $m_{k\Lambda} \approx 1710\,\mathrm{MeV}/c^2$. Fig. 11 shows the scattering amplitudes for the "lower region" with $m_{K\Lambda}^2 \in (2.9, 3.17)\,\mathrm{GeV}^2/c^4$ and the "upper region with $m_{K\Lambda}^2 \in (3.17, \infty)\,\mathrm{GeV}^2/c^4$. With the same method as described above we obtain we obtain $a_{\mathrm{eff}} = (-2.4 \pm 0.2)$ fm and $a_{\mathrm{eff}} = (-0.9 \pm 0.1)$ fm, respectively. This proves that N^* resonances lead to a dramatic systematic shift to smaller absolute scattering length. Therefore, it is necessary to study N^* resonances in more detail to make the method successful. A finer binning in $m_{K\Lambda}^2$ would give

important input for that but requires better statistics.

The theoretical predictions[9, 10, 11] for the scattering length are $a_s = -1.8\,\mathrm{fm}$ and $a_t = -2.4\,\mathrm{fm}$. Depending on the admixture of singlet and triplet scattering one expects a_{eff} to be between these values. If we interpret our result in the "upper region" as a limit on the scattering length this matches these predictions and would, in agreement with our findings on the K analyzing power, hint to the absence of spin triplet scattering. If, and only if, this is the case our result can also be compared to that of HIRES[12]. They obtain $a_s = -2.4^{+16}_{-0.25}$ with measurements of $pp \rightarrow pK\Lambda$ at $p_{\mathrm{beam}} = 2.7\,\mathrm{GeV}/c$. Even though the results are compatible in Ref.[13] it is shown that their method to determine the scattering length overestimates it by ≈ 0.4 fm. Furthermore, the influence of N^* resonances at their p_{beam} is unclear although earlier measurements of COSY-TOF[14] hint at weaker contributions.

6. Conclusion

COSY-TOF is able to measure the reaction $pp \rightarrow pK\Lambda$ with such a high reconstruction precision and efficiency that the experimental uncertainty of the determination of the $p\Lambda$ scattering length surpasses that of the employed method. However, with the complete kinematic acceptance we proved that the systematic effect of N^* resonances is the dominant uncertainty. This has to be understood in detail before one can precisely determine the $p\Lambda$ scattering length from final state interactions.

For the K analyzing power we found a decreasing contribution of S and P wave interference close to threshold. This was discussed in the context of exclusive spin singlet scattering. Even though our upper limit on the effective scattering length for $a_{\mathrm{eff}} = 2.4\,\mathrm{fm}$ fits into this picture we have to gather more data to give input for theoretical explanations of that effect.

We also determined the Λ depolarization to be ≈ -0.6 for forward Λ. This is in agreement with a previous result from the DISTO collaboration and hints to a prominent K exchange in the $pK\Lambda$ production mechanism. Incompatible results for backward Λs remain to be verified with better statistics.

7. Outlook

More beam times are already approved to improve statistics and measure at different beam momenta. This will improve the presented results and allow to study the influence of N^* resonances in more detail. At $p_{\mathrm{beam}} = 2.7\,\mathrm{GeV}/c^2$ a sample of $\approx$ 150.000 events was already collected. A first look into this data shows a Dalitz plot that is mostly described by $p\Lambda$ final state interactions and phasespace. The influence of N^* resonances seems to be modest, which is a clear advantage for the determination of a. Not only the the cusp effect has a strong energy dependence, but also A_N behaves differently. For low $m_{p\Lambda}$ preliminary results for p_1^1 are in the order of 15 %. This means that we might be able to determine a_t from this data.

References

[1] A. Gasparyan, J. Haidenbauer, C. Hanhart, J. Speth, How to extract the Lambda N scattering length from production reactions, Phys.Rev. C69 (2004) 034006. arXiv:hep-ph/0311116, doi:10.1103/PhysRevC.69.034006.

[2] M. Maggiora, New results from DISTO for spin observables in exclusive hyperon production, Nucl.Phys. A691 (2001) 329–335. doi:10.1016/S0375-9474(01)01053-3.

[3] M. Roeder, Final State Interactions and Polarization Variables in the Reaction $pp \rightarrow pK\Lambda$, Ph.D. thesis, Universitaet Bochum (2011).

[4] P. Wintz, A large tracking detector in vacuum consisting of self-supporting straw tubes, in: Intersections of Particle and Nuclear Physics: 8th Conference CIPANP2003, Vol. 698 of Issue 1, AIP Conf.Proc., 2004.

[5] S. Martin, G. Berg, U. Hacker, A. Hardt, M. Kohler, et al., COSY, a cooler synchrotron and storage ring, IEEE Trans.Nucl.Sci. 32 (1985) 2694–2696.

[6] D. Besset, B. Favier, L. Greeniaus, R. Hess, C. Lechanoine, et al., A set of efficient estimators for polarization measurements, Nucl.Instrum.Meth. 166 (1979) 515–520. doi:10.1016/0029-554X(79)90543-3.

[7] J. Laget, Strangeness production in nucleon-nucleon collisions, Phys.Lett. B259 (1991) 24–28. doi:10.1016/0370-2693(91)90127-C.

[8] D. Hutcheon, Measurements of $NN \rightarrow d\pi$ near threshold, TRI-PP-90-71.

[9] T. Rijken, V. Stoks, R. Klomp, J. De Kok, J. De Swart, The Nijmegen N N phase shift analyses, Nucl.Phys. A508 (1990) 173–184. doi:10.1016/0375-9474(90)90473-Y.

[10] J. Haidenbauer, U.-G. Meissner, The Julich hyperon-nucleon model revisited, Phys.Rev. C72 (2005) 044005. arXiv:nucl-th/0506019, doi:10.1103/PhysRevC.72.044005.

[11] H. Polinder, J. Haidenbauer, U.-G. Meissner, Hyperon-nucleon interactions: A Chiral effective field theory approach, Nucl.Phys. A779 (2006) 244–266. arXiv:nucl-th/0605050, doi:10.1016/j.nuclphysa.2006.09.006.

[12] A. Budzanowski, A. Chatterjee, H. Clement, E. Dorochkevitch, P. Hawranek, et al., High resolution study of the Lambda p final state interaction in the reaction $p + p \rightarrow K +$ +(*Lambdap*), Phys.Lett. B687 (2010) 31–35. arXiv:1003.0290, doi:10.1016/j.physletb.2010.02.082.

[13] A. Gasparyan, J. Haidenbauer, C. Hanhart, Extraction of scattering lengths from final-state interactions, Phys.Rev. C72 (2005) 034006. arXiv:nucl-th/0506067, doi:10.1103/PhysRevC.72.034006.

[14] S. Abd El-Samad, et al., Influence of N*-resonances on hyperon production in the channel $pp \rightarrow K + \Lambda p$ at 2.95, 3.20 and 3.30 GeV/c beam momentum, Phys.Lett. B688 (2010) 142–149. arXiv:1003.0603, doi:10.1016/j.physletb.2010.03.076.